



An ancient interleukin-16–like molecule regulates hemocyte proliferation *via* integrin β 1 in invertebrates

Received for publication, March 11, 2021, and in revised form, June 10, 2021. Published, Papers in Press, July 8, 2021.
<https://doi.org/10.1016/j.jbc.2021.100943>

Yue-Hong Zhao[‡], Hao Li[‡], Hui Zhao, Wei-Kang Sun, Qun Wang^{*ID}, and Wei-Wei Li^{*ID}

From the Laboratory of Invertebrate Immunological Defense & Reproductive Biology, School of Life Sciences, East China Normal University, Shanghai, China

Edited by Peter Cresswell

Interleukins (ILs) are cytokines with crucial functions in innate and adaptive immunity. IL genes are only found in vertebrates, except for IL-16, which has been cloned in some arthropod species. However, the function of this gene in invertebrates is unknown. In the present study, an IL-16–like gene (*EsIL-16*) was identified from the Chinese mitten crab *Eriocheir sinensis*. *EsIL-16* was predicted to encode a precursor (pro*EsIL-16*) that shares similarities with pro-IL-16 proteins from insects and vertebrates. We show that caspase-3 processes pro*EsIL-16* into an approximately 144-kDa N-terminal prodomain with nuclear import activity and an approximately 34-kDa mature peptide that might be secreted into the extracellular region. *EsIL-16* mRNA could be detected in all analyzed tissues and was significantly upregulated after immune challenge both *in vitro* and *in vivo*. T7 phage display library screening suggested potential binding activity between *EsIL-16* and integrin, which was confirmed by coimmunoprecipitation assay. Interestingly, *EsIL-16* promoted cell proliferation *via* integrin β 1 in primary cultured crab hemocytes and *Drosophila* S2 cells. Furthermore, the interaction between *EsIL-16* and integrin β 1 was necessary to efficiently protect the host from bacterial infection. To our knowledge, this study revealed integrin β 1 as a receptor for IL-16 and the function of this interaction in hemocyte proliferation in invertebrates for the first time. These results provide new insights into the regulation of innate immune responses in invertebrates and shed the light on the evolution of ILs within the animal kingdom.

It has become the central dogma of evolutionary immunologists that invertebrates, in the absence of “true” lymphocytes and functional antibodies, rely entirely on innate immunity as their primary mechanism of defense against parasites and pathogens (1). Arthropods, which comprise insects, crustaceans, and related forms, are a highly successful group of protostomate invertebrates about which a great deal is known concerning their immune systems and diseases (2). In general, arthropods use a range of cellular and humoral defenses to protect themselves from disease agents that

manage to gain access to their internal tissues by penetrating the exoskeleton/cuticle or alimentary canal (3). By contrast, vertebrates have both an acquired response and an innate system of defense; however, even within innate defense systems, extensive differences exist between vertebrates and invertebrates (4). For example, the interleukin (IL) superfamily members are cytokines produced and secreted mainly by CD3+ and CD4+ T lymphocytes, which promote development and differentiation of immune-related cells, are involved in systemic inflammation and immune system modulation, and thus play crucial roles in fighting infections and other diseases (5–7). To date, only a few *IL* genes have been traced evolutionarily back to invertebrates.

IL-16 is a cytokine originally designated as a lymphocyte chemoattractant factor and is characterized as an essential regulator of various cellular processes, including cell recruitment and activation (8, 9). IL-16 is generated as a precursor molecule (pro-IL-16) that appears to be predominantly produced by CD8+ and CD4+ T lymphocytes; however, other cells, including eosinophils, dendritic cells, mast cells, macrophages, B cells, and monocytes, also show high levels of IL-16 secretion under certain conditions (10, 11). IL-16 contains PDZ domains in the C-terminal region, which plays a key role in the formation and function of signal transduction, and might represent the signature of IL-16 molecules (12). IL-16 homologs have been well characterized in vertebrates, which show common functions associated with the recruitment of CD4+ or CD9+ immune cells to sites of inflammation, and function as the ligand for CD4 molecule (13–15). However, few reports have clarified the existence and function of IL-16 in arthropods. An IL-16–like gene was characterized and revealed to respond to bacteria and virus infection in shrimp (*Litopenaeus vannamei*) (16). Recently, pro-IL-16 was found to be cleaved to its bioactive form, mature IL-16, after bacterial challenge in crab (*Scylla paramamosain*) (17). Collective data verify the existence of IL-16 in arthropods; however, the immunological functions of this important molecule, as well as the receptor for IL-16 in arthropods and other invertebrates, still remain largely unclear.

Recent studies identified the expression pattern of *IL-16* in mud crab (17) and suggested that *IL-16* might regulate anti-bacterial immune responses positively in shrimp (16). The Chinese mitten crab (*Eriocheir sinensis*) represents a good

[‡] These authors contributed equally to this work.

^{*} For correspondence: Wei-Wei Li, wwli@bio.ecnu.edu.cn; Qun Wang, qwang@bio.ecnu.edu.cn.

Invertebrate IL-16 regulates hemocyte proliferation

model to study innate immunity within arthropods, mainly because of its clear genomic background (18, 19) and high commercial value (approximately US \$9.54 billion per year). In the present study, we identified an *IL-16-like* gene in Chinese mitten crab, demonstrated its induced expression after bacterial challenge, revealed the maturation process of pro-IL-16, and showed that mature IL-16 could promote hemocyte proliferation *via* interaction with its cell-membrane receptor, which indeed protected host from bacterial infection. These findings provide new insights into how IL-16 regulates innate immune responses in invertebrates and provide a better understanding of the evolution of ILs from invertebrates to vertebrates.

Results

Complementary DNA cloning and bioinformatics analysis of IL-16

The full-length *EsIL-16* complementary DNA (cDNA) was cloned from hemocytes of crab *E. sinensis*. The *EsIL-16* gene contains a short 5' UTR, a relatively long 3' UTR, and an ORF. The ORF was predicted to encode a 150.31-kDa protein comprising 1379 amino acids. The *EsIL-16* protein contains a potential caspase cleavage site and two PDZ domains at the C-terminal region (Fig. S1). After comparing the *EsIL-16* amino acid sequence with its homologs across vertebrates and invertebrates, comparatively high similarities were found among the C-terminal regions (Fig. 1A and Fig. S2), which comprise the mature IL-16 protein, suggesting that IL-16-regulated immunological functions might be partially conserved in different species. The PDZ domain acts as a signature for vertebrate IL-16 proteins, and analysis of the five vertebrate

and invertebrate species showed that IL-16 in vertebrates and its homolog IL-16-like protein in invertebrates carry a PDZ domain, mainly at the C terminus, which will be preserved in the mature IL-16 protein. However, mouse IL-16 has four PDZ domains located at the N terminus and C terminus, while the length of *Drosophila melanogaster* IL-16 amino acid sequence is obviously longer than that of the other species (Fig. 1B). Moreover, the IL-16 protein of *D. melanogaster*, *E. sinensis*, *Homo sapiens*, *Mus musculus*, and *Tetraodon nigroviridis* shared comparative similar structure (Fig. 1C). The phylogenetic analysis including numerous IL superfamily members from different vertebrate and invertebrate species showed *EsIL-16* clustered with IL-16 from other nine different species (Fig. 1D). However, IL-16 from fish *Fundulus heteroclitus* was not clustered with IL-16 from the other species, which indicate its different functions, but because of the limited information of IL-16 from *F. heteroclitus*, perhaps we cannot provide an explanation at this time.

Expression pattern of IL-16

The distribution of the *EsIL-16* mRNA in tissues was determined using quantitative RT-PCR (qRT-PCR) (Fig. 2A). *EsIL-16* expression was detected in all the examined tissues in *E. sinensis*. Among these tissues, hemocytes and heart expressed the lowest level of *EsIL-16*, whereas the hepatopancreas expressed the highest level, which was 30.7 times that in hemocytes. To test whether *EsIL-16* expression could be induced after challenge, *Staphylococcus aureus* and *Vibrio parahaemolyticus* were used to stimulate primary cultured crab hemocytes *in vitro* (Fig. 2, B and C) or infect crab *in vivo* (Fig. 2, D and E). The results showed significantly induced

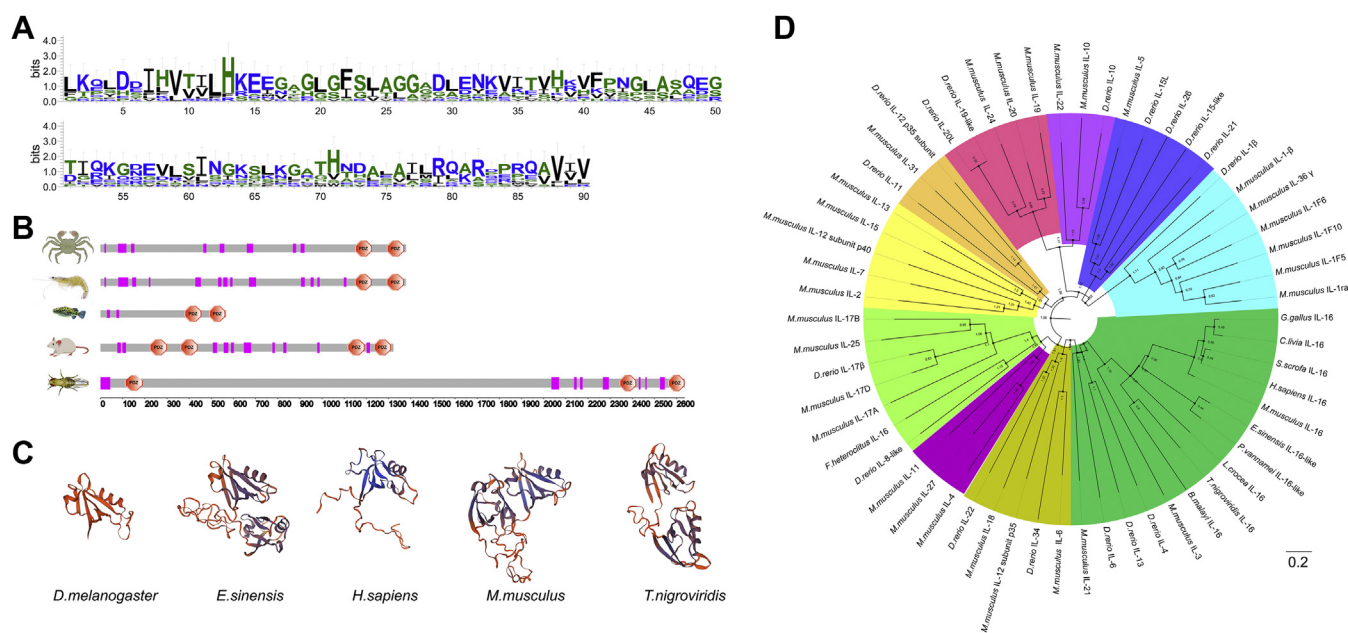


Figure 1. Pro-IL-16 domain architecture and protein structure. A, differential sequence conservation of IL-16. Sequence logo representation of the conservation of N-terminal region of pro-IL-16 from vertebrate and invertebrate species. Upper panel, bits (y-axis) indicate units of evolutionary conservation. B, diagram of the domain architectures of pro-IL-16 proteins from *Eriocheir sinensis*, *Penaeus vannamei*, *Tetraodon nigroviridis*, *Mus musculus*, and *Drosophila melanogaster*. C, a comparison of the 3D structures of pro-IL-16 proteins from aforementioned species. D, phylogenetic analysis of pro-IL-16 and some representative proteins from vertebrate and invertebrate species. The red star indicates *Es*-pro-IL-16, IL-16, interleukin 16.

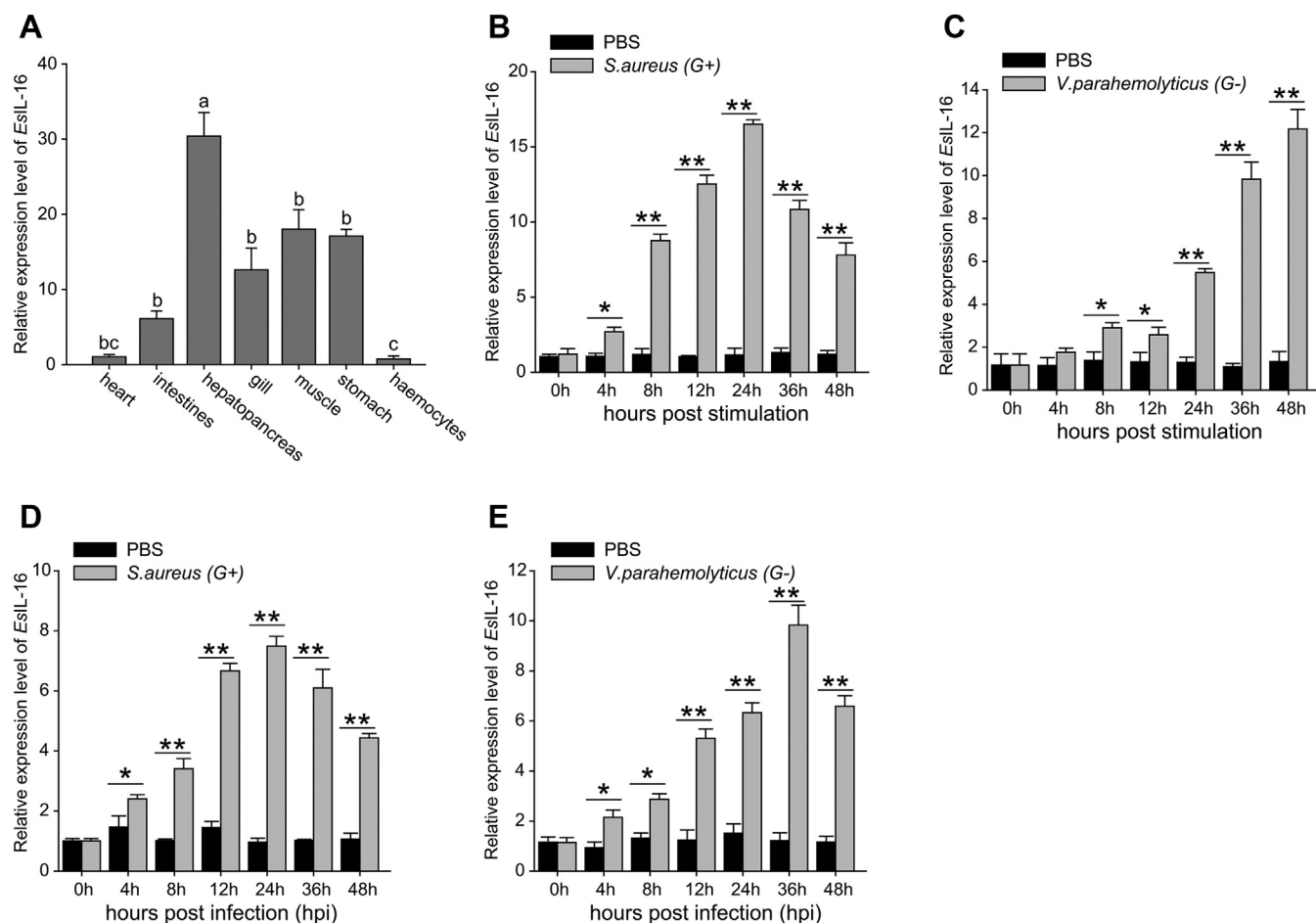


Figure 2. Expression pattern of IL-16. A, tissue distribution of IL-16. RNA samples were extracted from healthy *Eriocheir sinensis*, and *EsIL-16* expression was analyzed by quantitative RT-PCR with β -actin as the internal reference. Total RNA was extracted from seven different tissues of crab. Each sample was taken from at least three crabs; data shown are the means \pm SD. Three independent repeats were performed (≥ 5 crabs per sample), with different lowercase letters indicating the significance (one-way ANOVA). B–E, mRNA expression of *EsIL-16* in hemocytes as assessed by quantitative RT-PCR over a time course after *Staphylococcus aureus* (B) or *Vibrio parahemolyticus* (C) stimulation *in vitro* and *S. aureus* (D) or *V. parahemolyticus* (E) infection *in vivo*. RNA was extracted at 0, 4, 8, 12, 24, 36, and 48 h after bacterial challenge. Bars represent the mean \pm SD from three independent samples, with at least five crabs per sample. * $p < 0.05$, ** $p < 0.01$ (Student's *t* test). IL-16, interleukin 16.

EsIL-16 mRNA expression after challenge with both bacteria, thus demonstrating the potential participation of *EsIL-16* in innate immunity.

Detection of IL-16 cytoplasmic fragments and its nuclear or extracellular translocation

The vertebrate pro-IL-16 is cleaved by caspase-3 following cell activation into an N-terminal prodomain and a C-terminal peptide. The former can translocate into nuclei, whereas the latter is secreted from the cell to form mature IL-16 (20). However, whether the invertebrate IL-16-like protein shares a similar mechanism is unclear. Therefore, we screened the *EsIL-16* amino acid sequence and found a conserved nuclear localization signal in the N terminus that might have an essential role in IL-16 prodomain nuclear translocation and predicted a caspase cleavage site at the C terminus, cleavage of which might result in mature IL-16 release (Fig. 3A). After expressing N-terminal GFP-tagged and C-terminal hemagglutinin (HA)-tagged *Espro-IL-16* in human embryonic kidney

293T (HEK293T) cells, Western blotting using antibodies against the C-terminal HA showed that the *Espro-IL-16* protein comprised a prominent approximately 178-kDa fragment and a smaller fragment of 34 kDa (Fig. 3B), which coincided with the predicted molecular weight of *Espro-IL-16* and C-terminal mature IL-16, respectively. Meanwhile, Western blotting using antibodies against N-terminal GFP showed that the *Espro-IL-16* protein comprised a prominent approximately 178-kDa fragment as well as a smaller fragment of 144 kDa (Fig. 3C), which coincided with the predicted molecular weight of *Espro-IL-16* and the N-terminal *EsIL-16* prodomain, respectively. To detect the nuclear or extracellular translocation of *EsIL-16* fragments, we analyzed their subcellular localizations and quantified their protein content in the cytoplasm, nucleus, or cell culture medium of HEK293T cells. The 144-kDa N-terminal *EsIL-16* prodomain was found in the cytoplasm and nucleus, whereas the 34-kDa C-terminal mature *EsIL-16* was found only in the cytoplasm (Fig. 3D). Western blotting showed that increased *Escaspase-3* expression level in HEK293T cells led to upregulated cleavage

Invertebrate IL-16 regulates hemocyte proliferation

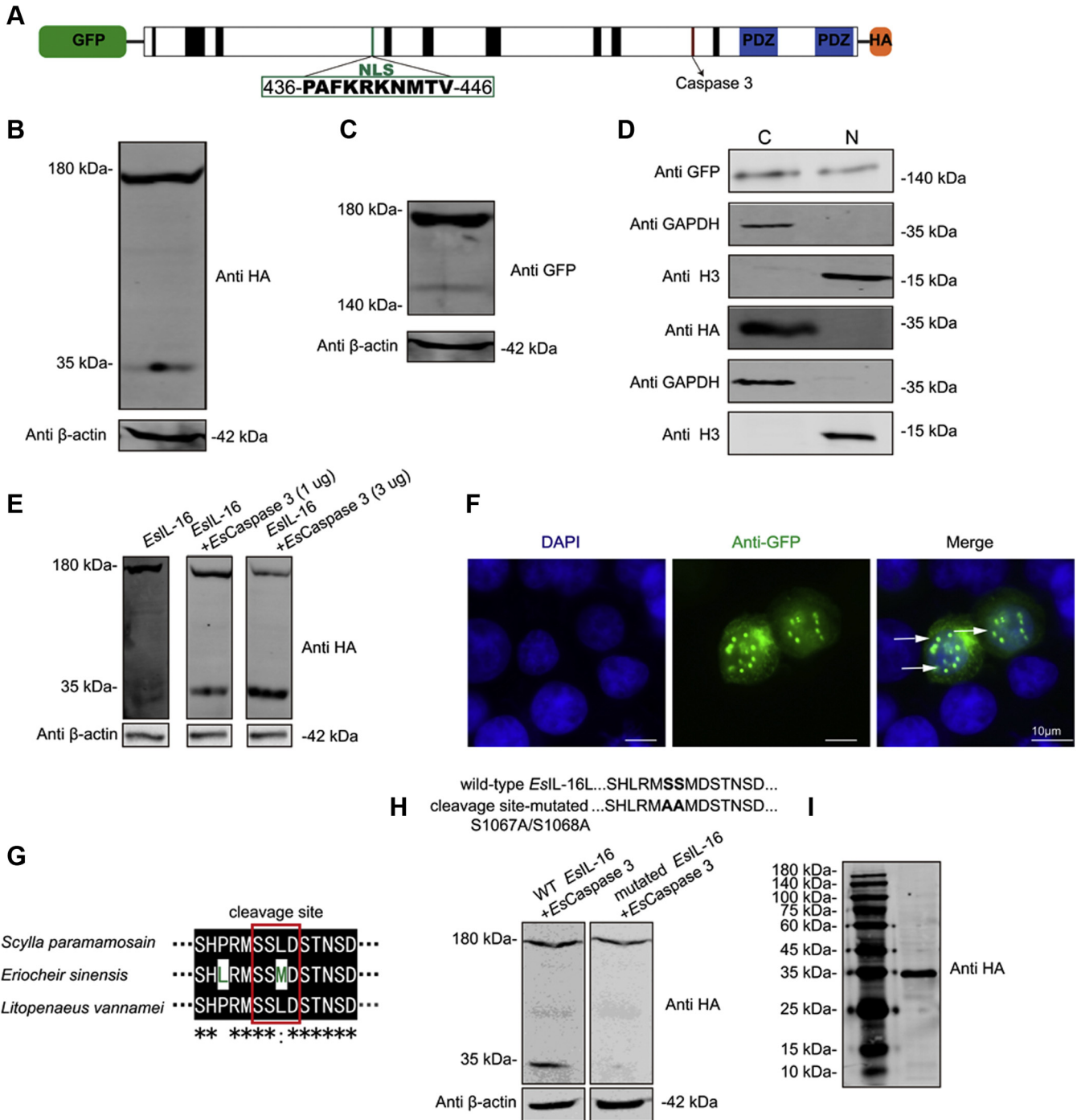


Figure 3. Caspase-dependent pro-IL-16 cleavage and secretion. *A*, schematic representation of HEK293T cells expressed N-terminal GFP-tagged and C-terminal HA-tagged pro-EsIL-16 protein. *B* and *C*, Western blotting showing the cleavage products of the (*B*) C-terminal FLAG-tagged mature EsIL-16 and (*C*) the N-terminal GFP-tagged EsIL-16 prodomain. *D*, Western blotting showed the N-terminal GFP-tagged EsIL-16 translocated into nuclei, rather than C-terminal FLAG-tagged mature EsIL-16. *E*, Western blotting showed that Escaspase-3 is responsible for EsIL-16 cleavage. Cells that only transfected with EsIL-16 cannot generate a small fragment, cells that cotransfected with EsIL-16 and low concentration (1 μ g) of Escaspase-3 generate clearly ~34 kDa small fragment, cells that cotransfected with EsIL-16 and high concentration (3 μ g) of Escaspase-3 generate a strong ~34 kDa fragment. *F*, immunostaining shown nuclear imported N-terminal GFP-tagged EsIL-16. *G*, sequence alignment between caspase-3 cleavage site from three crustacean species showed comparative similar regions between *Eriocheir sinensis* S1062 to D1075. *H*, mutated *E. sinensis* caspase-3 cleavage site with indicated point mutants that displayed in *bold* and named wildtype EsIL-16 and cleavage site-mutated, respectively (*upper panel*). Western blot analysis showed after Escaspase-3 (1 μ g) cotransfected with wildtype EsIL-16 or mutated EsIL-16, the wildtype EsIL-16 can generate a cleavage protein fragment with molecular weight of about ~34 kDa, but this fragment was absent in cleavage site-mutated EsIL-16 (*latter panel*). *I*, Western blotting showed that the C-terminal FLAG-tagged mature EsIL-16 is secreted into the extracellular region. Data are representative of three independent repeats. HA, hemagglutinin; HEK293T, human embryonic kidney 293T; IL-16, interleukin 16.

fragment of *EsIL-16* (Fig. 3E), and the immunostaining result showed that the *EsIL-16* prodomain localized to the nucleus (Fig. 3F). The alignment of amino acids between IL-16 from *E. sinensis* and the other two crustacean species demonstrated a conserved caspase cleavage site (Fig. 3G). After expressing the C-terminal HA-tagged wildtype *EsIL-16* and C-terminal HA-tagged cleavage site-mutated *EsIL-16* in HEK293T cells, the Western blot assay showed that the wildtype *EsIL-16* (178 kDa) can generate a small protein fragment with the molecular weight of about 34 kDa, but this band was not detected in cleavage site-mutated *EsIL-16* (Fig. 3H), which confirm the critical role of these amino acid residues in caspase cleavage, and also suggest the common features of caspase cleavage crustacean IL-16. Moreover, Western blotting revealed secreted mature *EsIL-16* in the cell culture medium of HEK293T cells (Fig. 3I).

Interaction between non-PDZ region of IL-16 and integrin beta subunits, N-terminal portion of extracellular region domain of integrin $\beta 1$

In vertebrates, the receptor of IL-16 has been identified as CD4 molecule (13–15); however, whole genome sequencing data suggested that there are no CD4 genes within insects (21) and crustacea (22), which indicated that IL-16 might bind with another, as yet unknown, cell-membrane receptor in invertebrates, which motivated us to screen for the IL-16 receptor in *E. sinensis*. After constructing a recombinant mature *EsIL-16* protein (Fig. 4B) that covered the region from the caspase 3 cleavage site to the end of the C terminus (Fig. 4A), a T7 phage display library expressing crab genes was used to screen potential *EsIL-16*-binding proteins. The results identified some possible binding proteins (Fig. 4C), with integrin $\beta 1$ and $\beta 2$ of particular interest because of their roles as cell-membrane receptors, as predicted by the transmembrane region by the TMHMM (Fig. S2) and the signal peptide by the signal-NM methods (Fig. S2).

To verify the potential interaction between *EsIL-16* and *Esintegrin* $\beta 1$ and $\beta 2$, we conducted coimmunoprecipitation (Co-IP) assays in HEK293T cells by expressing Flag-tagged mature *EsIL-16*, HA-tagged *Esintegrin* $\beta 1$, and HA-tagged *Esintegrin* $\beta 2$. The results showed that *EsIL-16* bound to *Esintegrin* $\beta 1$ rather than to *Esintegrin* $\beta 2$ (Fig. 4D). This result was confirmed by confocal analysis that *EsIL-16* colocalized with *Esintegrin* $\beta 1$ in HEK293T cells (Fig. 4E). To determine the role of the signature domains within *Esintegrin* $\beta 1$ for the protein-protein interaction, plasmids that expressed the extracellular region of *Esintegrin* $\beta 1$ and their truncated sequences were constructed (Fig. 4F) and expressed in HEK293T cells. Subsequently, Co-IP results showed that *EsIL-16* could bind to the integrin beta subunits, N-terminal portion of extracellular region domain of *Esintegrin* $\beta 1$ rather than the epidermal growth factor domain (Fig. 4G). To determine the role of the signature PDZ domains within *EsIL-16* for the protein-protein interaction, plasmids that expressed each or both PDZ domain were constructed (Fig. 4H) and expressed in HEK293T cells. Subsequently, Co-IP results showed that

Esintegrin $\beta 1$ could not bind with the PDZ domain of *EsIL-16* (Fig. 4I), which suggest that the N-terminal region of mature *EsIL-16* may act as the binding site for *Esintegrin* $\beta 1$.

Expression pattern of integrin $\beta 1$

The distribution of *Esintegrin* $\beta 1$ mRNA in tissues was determined using qRT-PCR (Fig. 5A). The expression of *Esintegrin* $\beta 1$ was detected in all examined tissues in *E. sinensis*. Among these tissues, hemocytes expressed a comparatively lower level of *Esintegrin* $\beta 1$, whereas hepatopancreas expressed the highest level, being 7.6 times higher than that in hemocytes. To test whether *Esintegrin* $\beta 1$ expression could be induced after challenge, *S. aureus* and *V. parahaemolyticus* were used to stimulate primary cultured hemocytes *in vitro* (Fig. 5, B and C) or infect crab *in vivo* (Fig. 5, D and E). The results showed significantly induced *Esintegrin* $\beta 1$ expression after challenge with both bacteria, thus suggesting its function in innate immunity.

IL-16 promotes cell proliferation via integrin $\beta 1$

The IL family members have important regulatory functions in cell differentiation and proliferation (6). Therefore, we carried out 5-ethynyl-2'-deoxyuridine (EdU) incorporation assays to assess whether cell proliferation in arthropod immune cells were controlled by IL-16 and integrin $\beta 1$. The expression of integrin $\beta 1$ in crab hemocytes was very low; therefore, hemocytes were pretreated with *S. aureus* to induce high expression of integrin $\beta 1$. After discarding the original cell culture medium and adding new medium without bacteria, recombinant IL-16 protein was added to the wildtype hemocytes or integrin $\beta 1$ -silenced hemocytes. The levels of EdU incorporation were analyzed at 12 and 48 h after stimulation (Fig. 6A). The results demonstrated that IL-16 significantly promoted hemocyte proliferation, whereas this phenotype was significantly suppressed in integrin $\beta 1$ -silenced hemocytes, which suggested that IL-16 promotes hemocyte proliferation *via* integrin $\beta 1$. To confirm the capacity of *EsIL-16* to promote cell proliferation *via* *Esintegrin* $\beta 1$, *Esintegrin* $\beta 1$ was stably expressed in S2 cells, and the cell proliferation regulated by *EsIL-16* was harvested and analyzed for carboxyfluorescein diacetate succinimidyl ester (CFSE) by flow cytometry (Fig. 6B). The results showed that *Esintegrin* $\beta 1$ -expressing S2 cells or *EsIL-16*-stimulated wildtype S2 cells did not show cell proliferation, whereas *Esintegrin* $\beta 1$ -expressing S2 cells that received *EsIL-16* stimulation had significantly induced CFSE signal peaks, which demonstrated that IL-16 could also promote S2 cell proliferation *via* integrin $\beta 1$.

IL-16-integrin $\beta 1$ protects the host from bacterial infection

To verify the role of the IL-16-integrin $\beta 1$ interaction in innate immunity, *siEsIL-16* (Fig. 7A) or *siEsintegrin* $\beta 1$ (Fig. 7B) was injected into crab hemolymph to knockdown their expression. A crab survival assay showed that *EsIL-16*- or *Esintegrin* $\beta 1$ -silenced crab has significantly suppressed survival rate after *S. aureus* (Fig. 7C) or *V. parahaemolyticus* (Fig. 7D) infection. Moreover, the two kinds of bacteria were

Invertebrate IL-16 regulates hemocyte proliferation

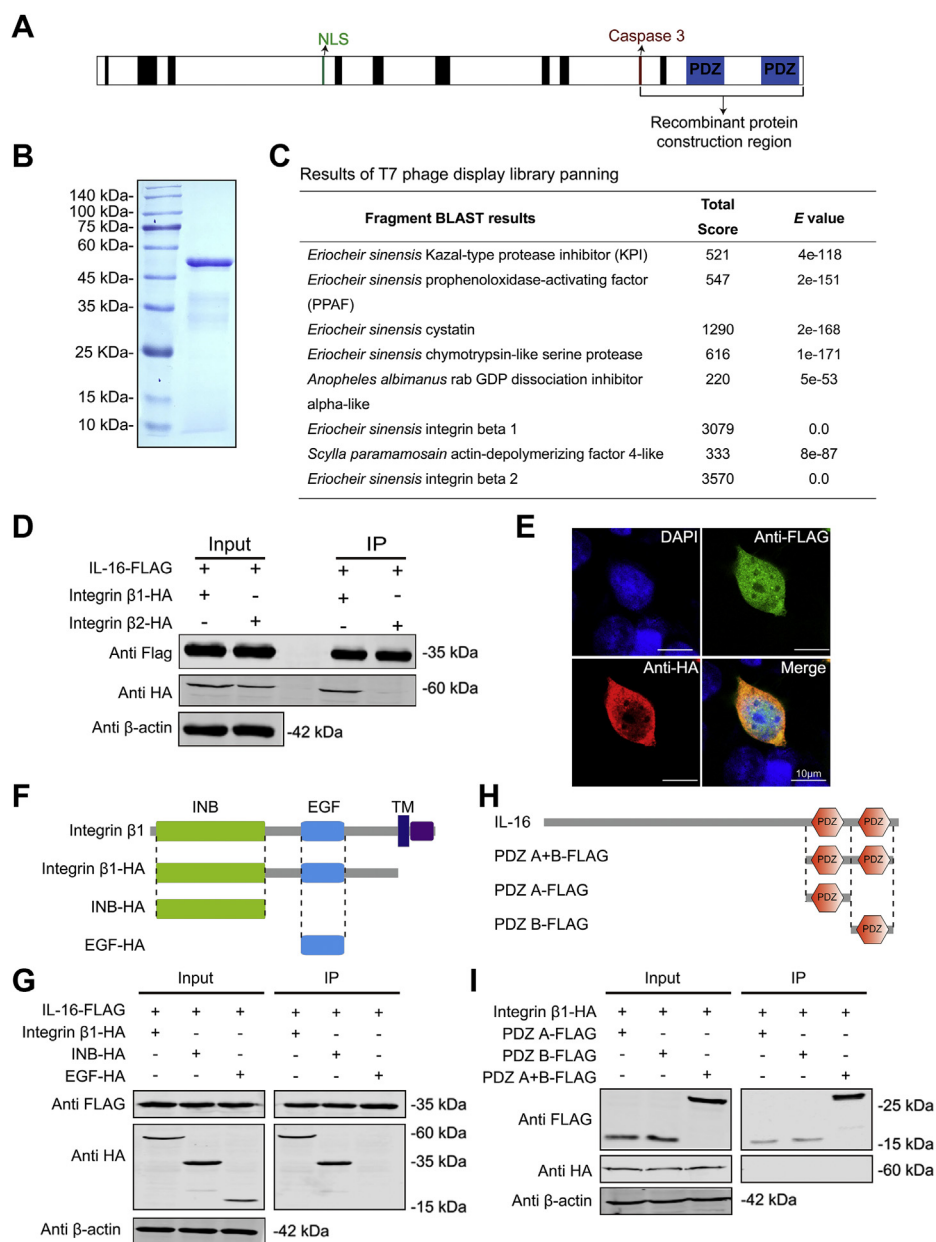


Figure 4. Interaction between IL-16 and integrin β 1. *A*, schematic diagram of regions ranging from the caspase 3 cleavage site to the last PDZ domain to construct the recombinant *EsIL-16* protein. *B* and *C*, recombinant *EsIL-16* protein (*B*)-based T7 phage library (*C*) screening suggesting the potential interaction between IL-16 and integrin β 1. Results for T7 phage library panning, two of eight sequenced fragments were identified as *Esintegrin* β 1/2 based on BLAST analysis. *D*, coimmunoprecipitation assay results showing the possible interaction between *Esintegrin* β 1, *Esintegrin* β 2, and mature *EsIL-16* in HEK293T cells. Anti-HA antibodies were used to detect *Esintegrin* β 1 or *Esintegrin* β 2, anti-Flag antibodies were used to detect *EsIL-16* in cotransfected HEK293T cells. The anti-HA and anti-FLAG antibodies were incubated with the cell lysates and then isolated using Protein G-FLAG-m-beads. *E*, colocalization of *EsIL-16* and *Esintegrin* β 1 in HEK293T cells by confocal analysis. *F*, illustration of different *Esintegrin* β 1 expression plasmids. *G*, coimmunoprecipitation assay results showing the interaction between different domains of *Esintegrin* β 1 and *EsIL-16* in HEK293T cells. Anti-FLAG and anti-HA antibodies were used to detect *EsIL-16* and *Esintegrin* β 1 in cotransfected HEK293T cells, respectively. *H*, illustration of different *EsIL-16* expression plasmids. *I*, coimmunoprecipitation assay results showing the interaction between different domains of *EsIL-16* and *Esintegrin* β 1 in HEK293T cells. Anti-FLAG and anti-HA antibodies were used to detect *EsIL-16* and *Esintegrin* β 1 in cotransfected HEK293T cells, respectively. Data are representative of three independent repeats. HA, hemagglutinin; HEK293T, human embryonic kidney 293T; IL-16, interleukin 16.

coated with r*EsIL-16*, in the presence or the absence of si*Esintegrin* β 1, and injected into crabs *in vivo*. A crab survival assay showed that r*EsIL-16* significantly improved survival rate of crabs after both *S. aureus* (Fig. 7E) or *V. parahaemolyticus* (Fig. 7F) infection in an *Esintegrin* β 1-dependent manner. Correspondingly, r*EsIL-16* significantly suppressed the hemolymph bacterial concentration in an *Esintegrin* β 1-dependent manner after *S. aureus* (Fig. 7G) or *V. parahaemolyticus*

(Fig. 7H) infection. These results suggested that the IL-16-integrin β 1 axis plays critical roles in innate immunity by promoting hemocyte proliferation *in vivo*.

Discussion

Cytokines are important factors to regulate the immune response and inflammation (23). As a proinflammatory

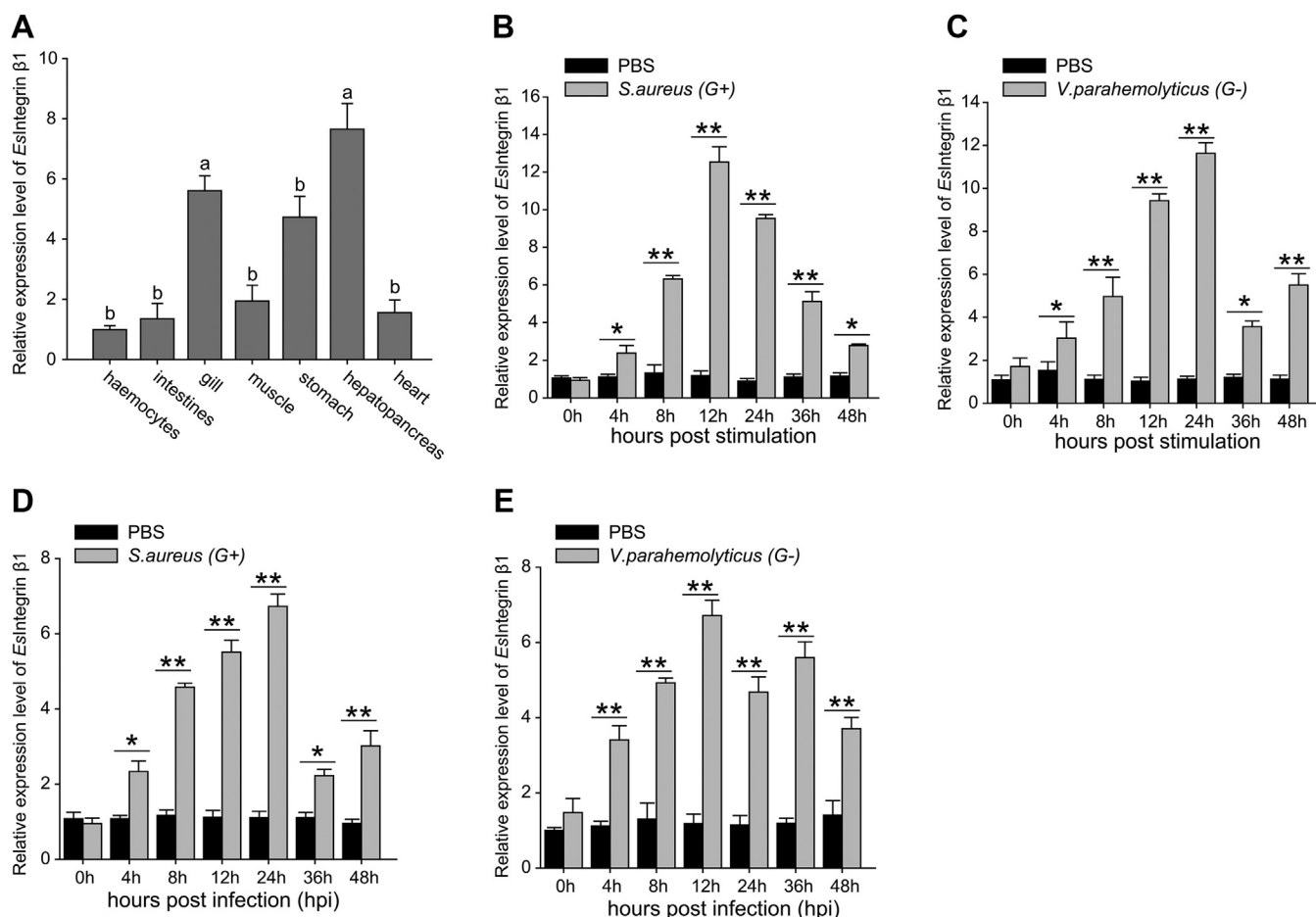


Figure 5. Expression pattern of *integrin* β 1. A, tissue distribution of *Esintegrin* β 1. RNA samples were extracted from healthy *Eriocheir sinensis*, and *Esintegrin* β 1 expression was studied by using quantitative RT-PCR with β -actin as the internal reference. Total RNA was extracted from seven different tissues of crab. Each sample was taken from at least three crabs. Data are shown as the means \pm SD. Three independent repeats were performed (≥ 3 crabs per sample), with different lowercase letters indicating the significance (one-way ANOVA). B–E, mRNA expression of *Esintegrin* β 1 in hemocytes was assessed using quantitative RT-PCR over a time course after *Staphylococcus aureus* (B) or *Vibrio parahaemolyticus* (C) stimulation *in vitro* and *S. aureus* (D) or *V. parahaemolyticus* (E) infection *in vivo*. RNA was extracted at 0, 4, 8, 12, 24, 36, and 48 h after bacterial challenge. The bars represent the mean \pm SD from three independent samples, with at least five crabs per sample. * $p < 0.05$, ** $p < 0.01$ (Student's *t* test).

cytokine, IL-16 plays a pivotal role in initiating innate and adaptive immune responses and assists in generating a local inflammatory response in vertebrates (8, 11). At present, *IL-16-like* genes have been widely predicted in the genomes of arthropods; however, currently, there are very limited data on the functional analyses of these genes (16, 17). Here, an *IL-16-like* gene was identified in crab, and its function in regulating hemocyte proliferation and in protecting the host from bacterial infection was revealed.

The amino acid sequences of the putative arthropod IL-16 proteins, in particular the C-terminal region, analyzed in this study share high similarities with each other. The C-terminal region of *EsIL-16* was highly homologous to those of the mature vertebrate IL-16 proteins, suggesting that IL-16 could be evolutionarily conserved within vertebrates and invertebrates. Interestingly, at present, IL-16-like genes have not been found in invertebrates other than arthropods, and thus, the evolutionary relationships between vertebrate and arthropod IL-16 genes and the reason why the IL-16 gene is absent in other phyla of invertebrates still remains unclear. In mammals, both

the lymphocyte-derived and neuronal IL-16 precursors are processed by caspase-3 to generate a mature IL-16 protein containing a single C-terminal PDZ domain (20). In contrast, *EsIL-16* has two PDZ domains in the C-terminal region, and bioinformatics analysis suggested that the potential caspase-3 cleavage site could be located before the first PDZ domain, indicating that processing by caspase-3 could generate a mature *EsIL-16* peptide containing two C-terminal PDZ domains. Our study showed that expression of the full-length *EsproIL16* cDNA in HEK293T cells also generated a 178-kDa band representing the N-terminal *EsIL-16* prodomain and a 34-kDa band representing the C-terminal mature *EsIL-16*, possibly as a result of caspase-3 cleavage, which has been confirmed in *L. vannamei* (16), and we also confirmed that caspase-3-mediated IL-16 cleavage in crab uncovered conserved amino acid residues between different crustacean species may act as a critical target for caspase cleavage. Moreover, the *EsIL-16* prodomain can translocate into the nucleus, and mature *EsIL-16* can be secreted into the extracellular region, which agreed with the results of studies in

Invertebrate IL-16 regulates hemocyte proliferation

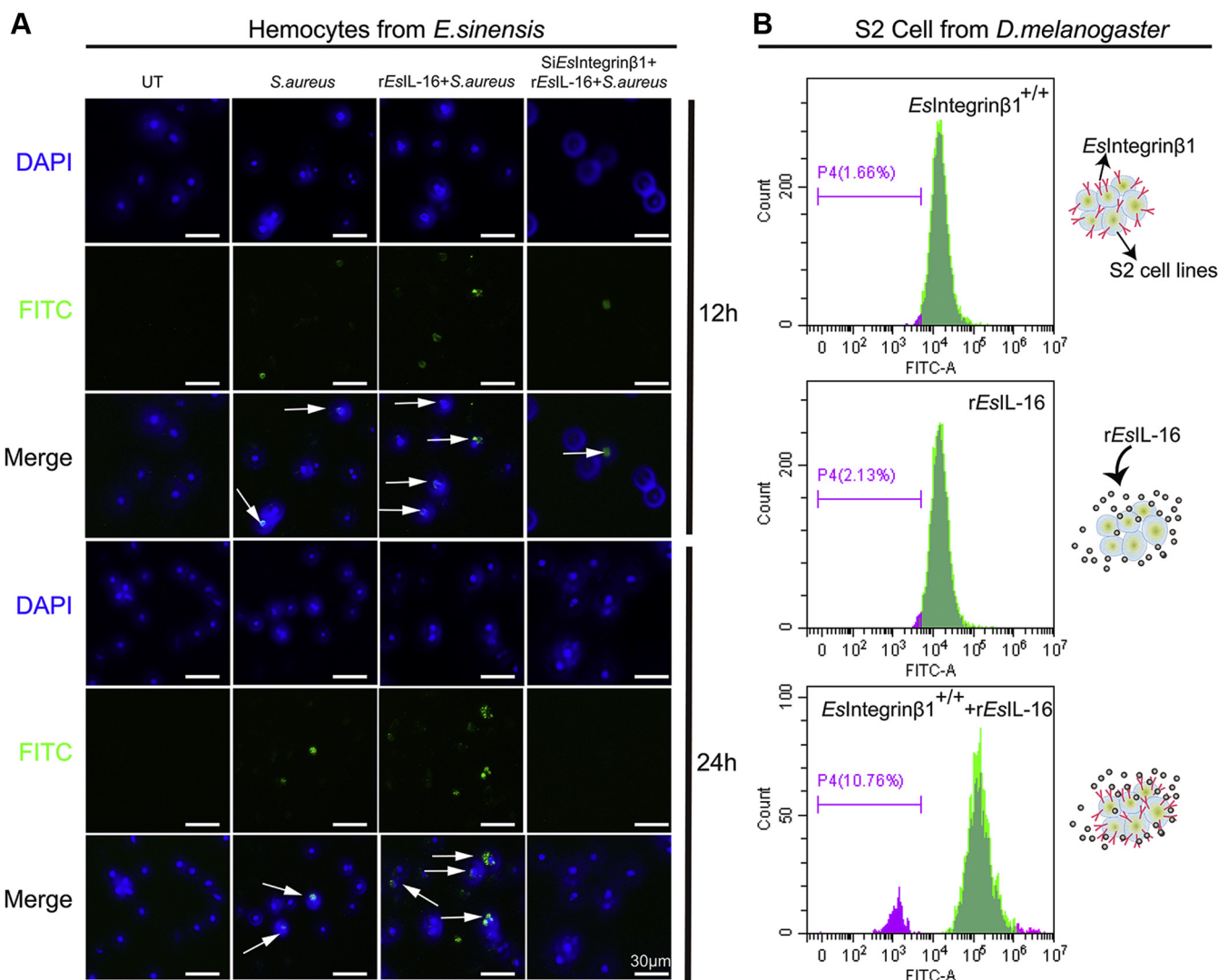


Figure 6. IL-16 promotes cell proliferation via integrin β 1 in different cell types. *A*, crab hemocytes proliferation detected by EdU labeling. EdU was applied to untreated hemocytes, *Staphylococcus aureus* stimulated hemocytes, *S. aureus* plus rEsIL-16 stimulated hemocytes, and *S. aureus* plus rEsIL-16 stimulated *EsIntegrin β 1-silenced hemocytes at time points indicated (12 and 48 h). Hemocytes were labeled anti-EdU (green) and anti-DAPI (blue). *B*, S2 cells proliferation monitored using CFSE labeling. CFSE was used to label the *EsIntegrin β 1-expressed S2 cells, rEsIL-16-stimulated S2 cells, or rEsIL-16-stimulated S2 cells that express *EsIntegrin β 1. After 24 h, cells were harvested and analyzed by flow cytometry. Cells at the right side represent nondivided CFSE-labeled responder cells, whereas the cells at the left side indicate daughter cell population that represent divided CFSE-labeled cells. Data are representative of three independent repeats. CFSE, carboxyfluorescein diacetate succinimidyl ester; DAPI, 4',6-diamidino-2-phenylindole dihydrochloride; EdU, 5-ethynyl-2'-deoxyuridine; IL-16; interleukin 16.***

vertebrates. Taken together, the aforementioned results suggested that although the lengths and domain compositions of the mature IL-16 products were different between arthropods and vertebrates, they employ similar processes to produce the mature protein.

In mammals, IL-16 modulates T cell-mediated inflammation via interaction with CD4 or CD9 in the target cell surface (13–15). However, genome sequencing data of *D. melanogaster* (21), *L. vannamei* (22), and *E. sinensis* (19) suggested that there is no *CD4* gene in the arthropod genome, *tsp2A* gene in *D. melanogaster* is a homolog of human CD9 (24), but there are no report on *tsp2A* in *E. sinensis*, and we could not find this gene in the genome database of *E. sinensis*. Thus, we speculated that another receptor might exist to bind arthropod IL-16 and activate downstream signal transduction.

Our study is the first to demonstrate the interaction between the transmembrane receptor integrin β 1 and IL-16 in invertebrates, which indicated that arthropod IL-16 might have different immune functions compared with those in mammals. Integrins are cell adhesion molecules that mediate cell–cell, cell–extracellular matrix, and cell–pathogen interactions (25). They play critical roles in the immune system, such as leukocyte trafficking and migration, immunological synapse formation, costimulation, and phagocytosis (25). Twenty-four integrin chains consisting of 18 alpha and eight beta subunits have been discovered in humans (26, 27), whereas only five alpha and two beta subunits have been found in fruit fly (28). Human immune cells express at least ten members of the integrin family, belonging to the β 2, β 7, and β 1 subfamilies, among which the β 2 and β 7 integrins are exclusively expressed

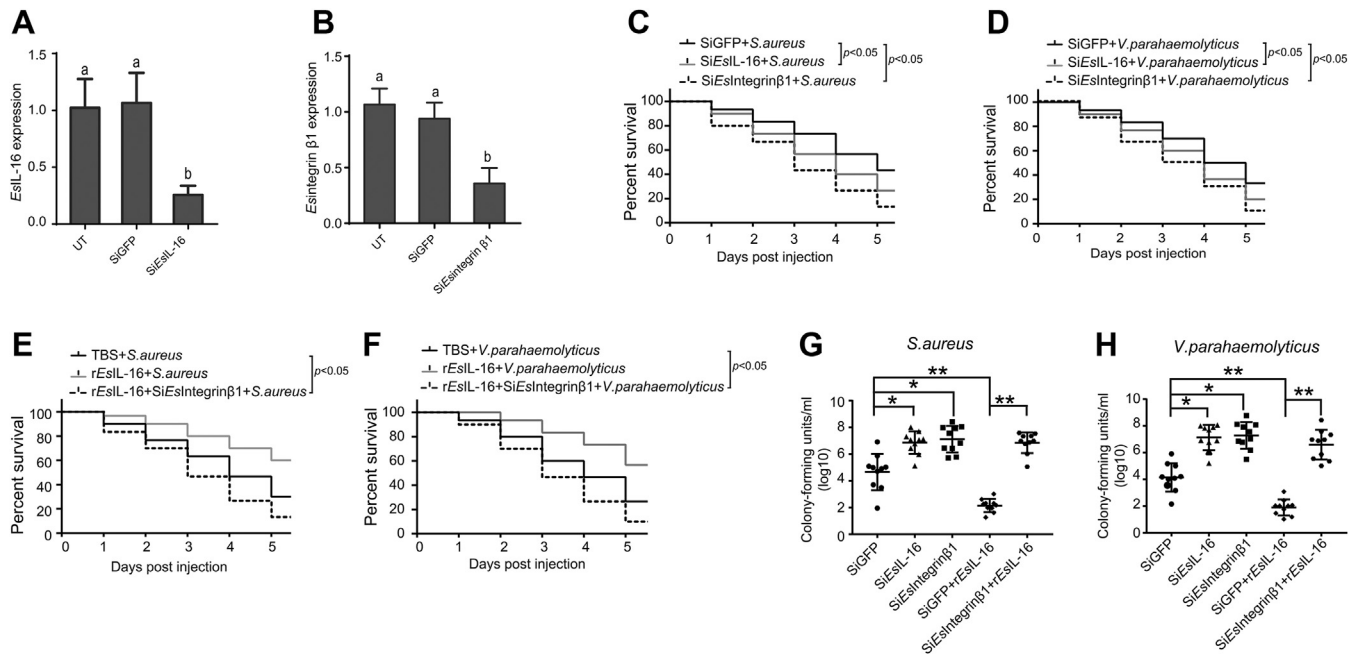


Figure 7. The IL-16-integrin $\beta 1$ axis protects crabs from bacterial infection. A, RNAi of the expression of *EsL-16* in crabs. B, RNAi of the expression of *Esintegrin $\beta 1$* in crabs. Each sample was taken from at least three crabs, and the results are shown as means \pm SD. Three independent repeats were performed (≥ 5 crabs per sample), with different lowercase letters indicating the significance (one-way ANOVA). C and D, *EsL-16* or *Esintegrin $\beta 1$* -silenced crabs showed increased susceptibility to *Staphylococcus aureus* and *Vibrio parahaemolyticus* infection. Crabs were each injected with si*EsL-16* or si*Esintegrin $\beta 1$* with siGFP as the control, and their 5-day survival post-*S. aureus* (C) and post-*V. parahaemolyticus* (D) infection was recorded from three independent repeats of 30 crabs per sample. E and F, *EsL-16* protects crabs from *S. aureus* or *V. parahaemolyticus* infection via *Esintegrin $\beta 1$* . Recombinant *EsL-16* was used to stimulate crabs, with or without si*Esintegrin $\beta 1$* , with TBS as the control, and their 5-day survival post-*S. aureus* (E) and post-*V. parahaemolyticus* (F) infection was recorded from three independent repeats of 30 crabs per sample. G and H, *EsL-16* reduces bacterial proliferation via *Esintegrin $\beta 1$* in crabs treated as described previously. From each crab, the hemolymph was drawn at day 4 post-*S. aureus* (G) and post-*V. parahaemolyticus* (H) infection and plated onto agar plates for bacterial counting. Shown are the means \pm SD. Three independent repeats were performed (≥ 10 crabs per sample). * $p < 0.05$, ** $p < 0.01$ (Student's *t* test). IL-16, interleukin 16; TBS, Tris-buffered saline.

on leukocytes, and the $\beta 1$ integrins are expressed on a wide variety of cells throughout the body. Nevertheless, their diversity in subunit composition contributes to the diversity in ligand recognition, binding to cytoskeletal components, and coupling to downstream signaling pathways (26, 27). Within invertebrate, integrin was first found in the hemocytes of the freshwater crayfish *Pacifastacus leniusculus* (29), and the later studies are focused on their multiple functions that include embryonic development, gut morphogenesis, and linkage of epithelia cells to extracellular matrix and cuticle (30). Furthermore, integrins have been proved to regulate the innate immune responses in invertebrates. For instance, *D. melanogaster* integrins play a key role in regulating cell adhesion and proliferation (31–33), whereas the β integrin domains from *Manduca sexta* and *Pseudoplusia* showed strong relationship with cell adhesion, encapsulation, and phagocytosis (34, 35). The interaction of IL-16 and integrin $\beta 1$ that was found in this study may suggest a different mechanism for IL-16 binding with the receptor between vertebrate and invertebrate and also may shed the light on integrin-regulated multiple immune responses in invertebrate.

Hemocytes play crucial roles in tissue remodeling during embryogenesis and metamorphosis and in immune defenses of arthropod. *Drosophila* contains three distinct hemocyte types including plasmatocytes, lamellocytes, and crystal cells, which generate distinct immune functions, such as antimicrobial peptide expression, encapsulation, phagocytosis, and

melanization (36). Significant progress has been made recently in understanding the genetic control of arthropod hemocyte differentiation during development (37). However, it is still unclear whether crustacean mature hemocytes have the ability to proliferate, whereas of course hematopoietic cells do (38–40), and information on the mechanisms by which hemocyte proliferation and differentiation are triggered during an immune response within invertebrate have so far remained elusive. Most other studies on hematopoiesis in insects demonstrated that maintenance of hemocyte populations during the larval stage also depends on both the proliferation of cells already in circulation and the release of hemocytes from hematopoietic organs. However, maintenance of mature hemocyte populations via proliferation of cells already in circulation appears to be more important during early stage of infection, whereas the production and release of hemocytes from the hematopoietic organs occurs delay. Several studies implicate Janus kinase/signal transducer and activator of transcription (41) and Pvr signaling (42) in the proliferation of prohemocytes, platelet-derived growth factor/vascular endothelial-like growth factor induces hemocyte proliferation in *Drosophila* larvae, and differentiation of prohemocytes into plasmatocytes, crystal cells, or lamellocytes requires down-regulation of Dome (43). The phenomenon of IL-16 promoting hemocyte proliferation by interacting with integrin $\beta 1$ has been revealed in this study; however, the downstream molecules, including transcription factors and effectors that

Invertebrate IL-16 regulates hemocyte proliferation

contribute to cell proliferation, still remain elusive, and identifying the key molecules that are activated by IL-16/integrin $\beta 1$ after pathogen infection requires further study.

In summary, under conditions of bacterial infection, the expression levels of IL-16 and integrin $\beta 1$ were significantly induced to activate immune reactions efficiently. Pro-IL-16 is cleavage by a caspase to generate an N-terminal IL-16 pro-domain and a C-terminal mature IL-16 peptide; the former may be translocated into the nucleus, whereas the latter will be secreted into the extracellular region. The secreted mature IL-16 interacts with the integrin beta subunits, N-terminal portion of extracellular region domain of integrin $\beta 1$, and this ligand/receptor interplay at the cell membrane could promote hemocyte proliferation by activating signaling transduction on the one hand and may induce antimicrobial peptide expression on the other hand (16), which has a synergistic action or an additive action to protect the host from bacterial infection.

Experimental procedures

Animals and primary cultured hemocytes

Healthy Chinese mitten crabs (*E. sinensis*, 100 \pm 10 g per adult) were purchased from the Songjiang aquatic farm. The crabs were transferred rapidly to the laboratory and maintained in aerated and filtered freshwater with an abundance of oxygen and fed daily with a commercially formulated antibiotic-free diet.

Primary culture of *E. sinensis* hemocytes was performed following established techniques (44). We collected hemolymph from the nonsclerotized membrane of the posterior walking leg using a 10-ml sterile syringe preloaded with 5 ml of precooled sterile anticoagulant (0.14 M NaCl, 0.1 M glucose, 30 mM trisodium citrate, 26 mM citric acid, 10 mM EDTA, and pH 4.6) at a ratio of 1:1. The hemolymph was centrifuged immediately at 300g at 4 °C for 10 min. The supernatant was removed, and the pellet was washed with PBS. The obtained hemocytes were resuspended gently in pure Leibovitz's L-15 medium (Sigma–Aldrich) containing 1% antibiotics (10,000 units/ml penicillin and 10,000 μ g/ml streptomycin; Gibco) and 0.2 mM NaCl (676 \pm 5.22 mOsm/kg), at pH 7.2 to 7.4, and then counted in an automated cell counter (Countess; Thermo Fisher Scientific). Then, 4 ml (1 \times 10⁶ cells/ml) were seeded in 60-mm dishes without any more additives.

D. melanogaster S2 cells were cultured in *Drosophila* Schneider's medium (Gibco) supplemented with 10% fetal bovine serum and antibiotics. HEK293T cells were cultured in Dulbecco's modified Eagle's medium (Life Technologies) in a humidified incubator at 37 °C and a 5% CO₂ atmosphere.

Protein annotation and phylogenetic analysis

The full-length cDNAs of encoding *EsIL-16* and *Esintegrin $\beta 1$* were amplified using gene-specific primers based on the sequences in National Center for Biotechnology Information and then resequenced to confirm their accuracy. Similarity analysis was performed using Clustalx from EMBL. SignalP, version 4.1 server (<http://www.cbs.dtu.dk/services/SignalP/>) and SMART (<http://smart.embl-heidelberg.de/>) were used to

predict the signal peptide and domain architecture, respectively. Swiss-PdbViewer (<https://spdbv.vital-it.ch/>) predicted the protein 3D structure. A phylogenetic tree was constructed based on the deduced amino acid sequences of *EsIL-16* and other known IL-16 within vertebrates and invertebrates (Table S2) using the neighbor-joining algorithm in MEGA (Mega Limited, Auckland, New Zealand), version 6.0 software, and bootstrap trials were replicated 1000 times.

Immune stimulation and sample collection

S. aureus and *V. parahaemolyticus* were obtained from the National Pathogen Collection Center for Aquatic Animals (nos. BYK0113 and BYK00036, respectively; Shanghai Ocean University). *S. aureus* is used commonly for bacterial infection in vertebrates and invertebrates, and *V. parahaemolyticus* is one of the most dangerous pathogens for aquatic animals (45). The two bacteria strains were cultured, collected, and resuspended in sterile PBS (137 mM NaCl, 2.7 mM KCl, 10 mM Na₂HPO₄, 2 mM KH₂PO₄, and pH 7.4). Bacterial counts were determined using the agar plating method.

In vitro and *in vivo* bacterial challenges were carried following a previously described method (46). For *in vitro* bacterial stimulation, cultured bacteria (1 \times 10⁷ cells per dish, 50 μ l) in 50 μ l sterile PBS were added separately to a hemocyte-culture dish to serve as the control. Total RNA was collected from hemocytes at specific time points after bacterial stimulation. At least three crabs were used per sample. First-strand cDNA was synthesized using a Reverse Transcriptase Kit (Takara) following the manufacturer's protocol. For *in vivo* bacterial infection, bacteria (1 \times 10⁸ colony-forming units per crab, 200 μ l) were injected into the hemolymph from the nonsclerotized membrane of a posterior walking leg that differed from the site for hemolymph collection; sterile PBS (200 μ l) was used injected as the control. Total RNA was collected from hemocytes at specific time points after infection. At least three crabs were used per sample.

RNAi assay

The cDNA fragments of *EsIL-16* and *Esintegrin $\beta 1$* were first amplified using PCR with primers containing a T7 promoter (Table S1). The cDNAs were then used as the templates to produce siRNA using an *in vitro* T7 Transcription Kit (Fermentas). The corresponding control GFP siRNA was purchased from GenePharma. For *in vitro* RNAi, the siRNAs were dissolved in RNase-free water and transfected into *E. sinensis* primary-cultured hemocytes with the aid of 10 nM Lipofectamine 3000 (Thermo Fisher Scientific). For *in vivo* RNAi, the siRNAs (1 μ g/g) were injected into hemolymph from the nonsclerotized membrane of the posterior walking leg of each crab. The RNAi efficiency was assessed using real-time qRT-PCR, with double-stranded GFP RNA as the control. After setting up the RNAi assay, *S. aureus* was used to stimulate the gene-silenced hemocytes *in vitro*, and *S. aureus* or *V. parahaemolyticus* was used to infect the gene-silenced crabs *in vivo*.

Gene expression profile analysis

The relative gene expression levels in treated hemocytes were determined using qRT-PCR and SYBR Premix Ex Taq (Tli RNaseH Plus) and the CFX96 Real-Time System (Bio-Rad) and with gene-specific primers (Table S1). The reaction conditions comprised 94 °C for 3 min; followed by 40 cycles of 94 °C for 10 s and 60 °C for 1 min; and then melting curve analysis from 65 to 95 °C. The $2^{-\Delta\Delta CT}$ method was used to normalize the obtained data to that of the control group. Three independent experiments were conducted, with results expressed as the mean \pm SD.

Western blotting

Protein samples obtained from HEK293T cells were quantified using the Coomassie Plus protein assay reagent (Thermo Fisher Scientific). HEK293T cells were lysed in radioimmunoprecipitation assay lysis buffer (50 mM Tris, pH 7.4, 150 mM NaCl, 1% NP-40, 0.25% sodium deoxycholate, sodium orthovanadate, sodium fluoride, EDTA, and leupeptin) containing protease and phosphatase inhibitor mixtures (Roche Applied Science). Cytoplasmic and nuclear proteins were extracted using a Nuclear Protein Extraction Kit (Beyotime) according to the manufacturer's instructions. Protein concentrations were quantified using a Pierce BCA Protein Assay Kit (Thermo Fisher Scientific). The proteins were then separated using 10% SDS-PAGE and then transferred to a nitrocellulose membrane. The membrane was blocked for 1 to 2 h using 3% nonfat milk in Tris-buffered saline (TBS) (10 mM Tris-HCl, pH 8.0, 150 mM NaCl) and then incubated with commercial antibodies against HA, GAPDH, histone H3, GFP, the Flag tag, or β -actin (all from Abcam) in TBS-3% nonfat milk for 3 h. The membrane was washed three times in TBS, and alkaline phosphatase-conjugated goat anti-rabbit/antimouse IgG (1:10,000 dilution in TBS) was added and incubated for 3 h, followed by washing to remove the unbound IgG. The membrane was incubated with the reaction system and visualized in the dark using 4-chloro-1-naphthol oxidation for 5 min. All images were captured using the Odyssey CLx system (LI-COR).

Immunocytochemical staining

Immunocytochemical staining was used to examine the subcellular location of the N-terminal *EsIL-16* prodomain in HEK293T cells. Briefly, pretreated cells were blocked with 3% bovine serum albumin (BSA) for 30 min at 37 °C and then incubated with antibodies recognizing GFP-tagged *EsIL-16* overnight at 4 °C. After washing with PBS, the cells were incubated with 3% BSA for 10 min, after which the goat antimouse Alexa Fluor 488 secondary antibody (1:1000 dilution in 3% BSA) was added. The reaction was performed in the dark for 1 h at 37 °C, and then the cells were washed with PBS. Finally, the cells were stained with 4',6-diamidino-2-phenylindole dihydrochloride (Anaspec) for 10 min at room temperature, washed, and observed under a Revolve Hybrid Microscope (Echo).

Panning of the T7 phage display library

Panning was performed based on previously published method (47) with some modifications. Briefly, 40 μ g of purified mature *EsIL-16* protein was added to the wells of a 96-well plate and incubated at 4 °C overnight. The unbound protein was removed by washing with PBS twice, and 10 μ l of T7 phage display library derived from Chinese mitten crab hemocytes was added to the wells. Incubation was performed overnight. After three washes with TBST (50 mM Tris-HCl, 0.5 M NaCl, 0.02% Tween 20, and pH 7.5), *EsIL-16*-bound phages were eluted using 200 μ l of 1% SDS and then centrifuged at 6000g for 5 min. Then, 10 μ l of the supernatant was inoculated into 1 ml of BLT5403 cell culture (absorbance at 600 nm = 0.5) and cultured at 37 °C for 2 h. The culture was centrifuged, and the supernatant was plated on an agarose plate containing the BLT5403 cells. The plates were cultured at 37 °C for 3 h. Extraction buffer (100 mM NaCl, 6 mM MgSO₄, 20 mM Tris-HCl, and pH 8.0) was added to the wells, and the plates were incubated at 4 °C overnight. The extraction buffer was then collected for the next panning. After three repeats, single plaques appeared, and the ten longest (>500 bp) fragments were sequenced.

Co-IP

A Co-IP assay was performed according to a previously described method (44) to detect the interaction between *EsIL-16* and *Esintegrin* β 1. HEK293T cells were seeded in 60-mm dishes (1 \times 10⁷ cells/dish) overnight and transfected with 10 mg of empty plasmid or various expression plasmids. At 48 h posttransfection, the medium was removed carefully, and the cell monolayer was washed twice with ice-cold PBS. The cells were then lysed using 500 μ l of radioimmunoprecipitation assay lysis buffer (Beyotime) containing a protease cocktail (Yeasen). Lysates were centrifuged at 14,000g for 15 min. The supernatant was transferred to a fresh tube and precipitated for 2 h at 4 °C with 30 μ l of either an anti-HA or anti-Flag affinity gel (Biotool). The affinity gel was washed with cold TBS four times and eluted by boiling for 10 min in TBS and a 6 \times SDS loading buffer (2% SDS, 60 mM Tris-HCl, pH 6.8, 10% glycerol, 0.001% bromophenol blue, and 0.33% 2-mercaptoethanol). The cell lysates were also eluted using this 6 \times SDS loading buffer and boiled. Proteins isolated from the beads and cell lysates were separated using SDS-PAGE and analyzed by Western blotting using the indicated antibodies. All images were captured by the Odyssey CLx system (LI-COR).

Laser scanning confocal analysis

Confocal was used to examine the possible interaction between *EsIL-16* and *Esintegrin* β 1. HEK293T cells were seeded onto 24 \times 24 mm glass cover slips in 35-mm dishes overnight and transfected with 1 μ g of empty or expression plasmids. At 36 h after transfection, the medium was removed and the cells were washed twice with PBS and fixed immediately with 4% paraformaldehyde in sterile PBS for 15 min. The cells were then permeabilized with 0.5% Triton X-100 in PBS for 10 min,

Invertebrate IL-16 regulates hemocyte proliferation

washed with PBS three times, and blocked with 3% BSA for 2 h and then incubated with anti-Flag antibody (1:200) and anti-HA antibody (1:200) overnight at 4 °C. Subsequently, unbound antibody was removed by washing with PBS with Tween-20 (PBST), cells were stained with goat IgG H&L (FITC conjugated) (1:100) and goat anti-rabbit IgG H (Rhodamine Red-X conjugated) (1:100) for 2 h at 37 °C. After washing with PBST, cells were stained with 4',6-diamidino-2-phenylindole dihydrochloride for 5 min. After a final wash in PBST, cover slips were sealed with nail polish on the edges and then removed for observation under a laser scanning confocal microscope (Leica).

Recombinant expression and purification

A PCR fragment representing the mature *EsIL-16* was amplified using specific primers (Table S1). Subsequently, the PCR products were purified, digested with restriction enzymes (EcoRI and XhoI), and ligated into the pET-28a (+) vector (Novagen). The recombinant plasmid pET-28a (+)-*EsIL-16* was transformed into *Eriochair coli* Rosetta (DE3) cells (Transgene) for expression of the recombinant mature *EsIL-16* protein. Fusion protein expression was induced using four different sets of conditions: 1 mM IPTG for 3 h at 37 °C; 0.25 mM IPTG for 3 h at 37 °C; 1 mM IPTG for 3 h at 30 °C; and 0.25 mM IPTG for 3 h at 30 °C. The fusion protein was purified using nickel-nitrilotriacetic acid resin (Transgene) according to the manufacturer's instructions.

Cell proliferation

Crab hemocyte and S2 cell proliferation was detected using the EdU and CFSE methods, respectively. EdU incorporation was analyzed according to the manufacturer's instructions using the Click-iT Plus EdU Imaging Kit (Life Technologies). Briefly, half of the cell culture media was replaced with fresh media containing 20 μM EdU and incubated for another 24 h. Cells were fixed with formaldehyde, permeabilized with 0.5% Triton X-100, and stained with a reaction cocktail and Hoechst according to the manufacturer's instructions. Cells were imaged with fluorescence microscopy, and the percentage of EdU-positive cells was evaluated by fluorescence microscopy. For the CFSE method, a CFSE stock solution was prepared (10 mM in dimethyl sulfoxide; Invitrogen) and stored at -20 °C. The stock solution was thawed and diluted in PBS to the desired working concentrations. In pilot experiments, we tested different CFSE labeling conditions (final concentrations: 0.2, 0.5, 1, 2, 5, and 10 μM) to obtain a high cell viability and a broad CFSE signal measurement toward antigen or polyclonal stimuli. S2 cells were resuspended in PBS (with 0.1% BSA) at 2×10^6 cells/ml and incubated with CFSE (final concentration: 1 μM) for 7 min at 37 °C. The cells were washed and resuspended in culture medium for 15 min to stabilize the CFSE staining. After a final wash step, the cells were resuspended in culture medium at the indicated cell concentrations. Thereafter, the CFSE-labeled S2 cells were transfected with the *Esintegrin* β1 overexpression plasmid with or without *EsIL-16* (200 ng/ml; 100 μl) stimulation. After 48 h,

the S2 cells were harvested, and the CFSE signal of gated cells was analyzed using flow cytometry (Beckman).

Assessment of crab survival and bacterial clearance assay

Crabs were divided randomly into eight groups of 30 animals each. After pretreatment with the *EsIL-16* siRNA, *Esintegrin* β1 siRNA, GFP siRNA, recombinant *EsIL-16* protein, *Esintegrin* β1 siRNA plus the recombinant *EsIL-16* protein or TBS, all crabs were injected with *S. aureus* or *V. parahaemolyticus* (1×10^9 colony-forming units per crab, 200 μl). Dead crabs in each group were counted daily, and survival was tabulated over 5 days. Four days after the bacterial injections, the hemolymph from each crab was collected, diluted, and cultured overnight on solid LB plates, and then the bacterial colonies on each plate were counted.

Data availability

All data are contained within the article.

Supporting information—This article contains [supporting information](#).

Acknowledgments—We thank the Experimental Platform for Molecular Zoology (East China Normal University, Shanghai, China) for providing instruments essential for conducting our study.

Author contributions—Y.-H. Z. data curation; Y.-H. Z., H. L., and W.-W. L. validation; Y.-H. Z., H. L., H. Z., W.-K. S., W.-W. L. investigation; Y.-H. Z. and H. L. visualization; Y.-H. Z., H. L., H. Z., and W.-K. S. methodology; Y.-H. Z. and W.-W. L. writing—original draft; Q. W. and W.-W. L. funding acquisition; Q. W. and W.-W. L. project administration; W.-W. L. conceptualization; W.-W. L. supervision.

Funding and additional information—This work was supported by the National Natural Science Foundation of China (Grants 31972820 to W.-W. L. and 31970490 to Q. W.) and Shanghai Rising-Star Program (Grant 20QA1403000 to W.-W. L.).

Conflict of interest—The authors declare that they have no conflicts of interest with the contents of this article. All authors agree with the submission. This work has not been published or submitted for publication elsewhere, either completely or in part, or in another form or language. No material has been reproduced from another source. Experiments using invertebrate animal were approved by local authorities.

Abbreviations—The abbreviations used are: BSA, bovine serum albumin; cDNA, complementary DNA; CFSE, carboxyfluorescein diacetate succinimidyl ester; Co-IP, coimmunoprecipitation; EdU, 5-ethynyl-2'-deoxyuridine; HA, hemagglutinin; HEK293T, human embryonic kidney 293T; IL, interleukin; PBST, PBS with Tween-20; qRT-PCR, quantitative RT-PCR; TBS, Tris-buffered saline.

References

1. Little, T. J., Hultmark, D., and Read, A. F. (2005) Invertebrate immunity and the limits of mechanistic immunology. *Nat. Immunol.* **6**, 651–654

2. Buchon, N., Silverman, N., and Cherry, S. (2014) Immunity in *Drosophila melanogaster*—from microbial recognition to whole-organism physiology. *Nat. Rev. Immunol.* **14**, 796–810
3. Rowley, A. F., and Powell, A. (2007) Invertebrate immune systems specific, quasi-specific, or nonspecific? *J. Immunol.* **179**, 7209–7214
4. Hoffmann, J. A., Kafatos, F. C., Janeway, C. A., and Ezekowitz, R. A. (1999) Phylogenetic perspectives in innate immunity. *Science* **284**, 1313–1318
5. Brocker, C., Thompson, D., Matsumoto, A., Nebert, D. W., and Vasilidou, V. (2010) Evolutionary divergence and functions of the human interleukin (IL) gene family. *Hum. Genomics* **5**, 30–55
6. Dinarello, C. A., and Mier, J. W. (1986) Interleukins. *Annu. Rev. Med.* **37**, 173–178
7. Secombes, C. J., Wang, T., and Bird, S. (2011) The interleukins of fish. *Dev. Comp. Immunol.* **35**, 1336–1345
8. Cruikshank, W., and Center, D. M. (1982) Modulation of lymphocyte migration by human lymphokines. II. Purification of a lymphotactic factor (LCF). *J. Immunol.* **128**, 2569–2574
9. Richmond, J., Tuzova, M., Cruikshank, W., and Center, D. (2014) Regulation of cellular processes by interleukin-16 in homeostasis and cancer. *J. Cell. Physiol.* **229**, 139–147
10. Conti, P., Kempuraj, D., Kandere, K., Di Gioacchino, M., Reale, M., Barbacane, R. C., Castellani, M. L., Mortari, U., Boucher, W., Letourneau, R., and Theoharides, T. C. (2002) Interleukin-16 network in inflammation and allergy. *Allergy Asthma Proc.* **23**, 103–108
11. Sharma, V., Sparks, J. L., and Vail, J. D. (2000) Human B-cell lines constitutively express and secrete interleukin-16. *Immunology* **99**, 266–271
12. Ponting, C. P. (1997) Evidence for PDZ domains in bacteria, yeast, and plants. *Protein Sci.* **6**, 464–468
13. Cruikshank, W., and Little, F. (2008) Interleukin-16: The ins and outs of regulating T-cell activation. *Crit. Rev. Immunol.* **28**, 467–483
14. Liu, C., Mills, J., Dixon, K., Vennarini, J., Cunningham, M., Del Vecchio, A., Das, A., and Glass, W. (2007) IL-16 signaling specifically induces STAT6 activation through CD4. *Cytokine* **38**, 145–150
15. Skundric, D. S., Cai, J., Cruikshank, W. W., and Gveric, D. (2006) Production of IL-16 correlates with CD4+ Th1 inflammation and phosphorylation of axonal cytoskeleton in multiple sclerosis lesions. *J. Neuroinflammation* **3**, 13
16. Liang, Q., Zheng, J., Zuo, H., Li, C., Niu, S., Yang, L., Yan, M., Weng, S. P., He, J., and Xu, X. (2017) Identification and characterization of an interleukin-16-like gene from pacific white shrimp *Litopenaeus vannamei*. *Dev. Comp. Immunol.* **74**, 49–59
17. Gu, W. B., Zhou, Y. L., Tu, D. D., Zhou, Z. K., Zhu, Q. H., Chen, Y. Y., and Shu, M. A. (2017) Identification and characterization of pro-interleukin-16 from mud crab *Scylla paramamosain*: The first evidence of proinflammatory cytokine in crab species. *Fish Shellfish Immunol.* **70**, 701–709
18. Song, L., Bian, C., Luo, Y., Wang, L., You, X., Li, J., Qiu, Y., Ma, X., Zhu, Z., Ma, L., Wang, Z., Lei, Y., Qiang, J., Li, H., Yu, J., et al. (2016) Draft genome of the Chinese mitten crab, *Eriocheir sinensis*. *Giga-science* **5**, 5
19. Tang, B., Wang, Z., Liu, Q., Zhang, H., Jiang, S., Li, X., Wang, Z., Sun, Y., Sha, Z., Jiang, H., Wu, X., Ren, Y., Li, H., Xuan, F., Ge, B., et al. (2019) High-quality genome assembly of *Eriocheir japonica sinensis* reveals its unique genome evolution. *Front. Genet.* **10**, 1340
20. Zhang, Y., Center, D. M., Wu, D. M., Cruikshank, W. W., Yuan, J., Andrews, D. W., and Kornfeld, H. (1998) Processing and activation of pro-interleukin-16 by caspase-3. *J. Biol. Chem.* **273**, 1144–1149
21. Myers, E. W., Sutton, G. G., Delcher, A. L., Dew, I. M., Fasulo, D. P., Flanigan, M. J., Kravitz, S. A., Mobarry, C. M., Reinert, K. H., Remington, K. A., Anson, E. L., Bolanos, R. A., Chou, H. H., Jordan, C. M., Halpern, A. L., et al. (2000) A whole-genome assembly of *Drosophila*. *Science* **287**, 2196–2204
22. Zhang, X., Yuan, J., Sun, Y., Li, S., Gao, Y., Yu, Y., Liu, C., Wang, Q., Lv, X., Zhang, X., Ma, K. Y., Wang, X., Lin, W., Wang, L., Zhu, X., et al. (2019) Penaeid shrimp genome provides insights into benthic adaptation and frequent molting. *Nat. Commun.* **10**, 356
23. Neurath, M. F. (2014) Cytokines in inflammatory bowel disease. *Nat. Rev. Immunol.* **14**, 329–342
24. Jeibmann, A., Halama, K., Witte, H. T., Kim, S. N., Eikmeier, K., Koos, B., Klämbt, C., and Paulus, W. (2015) Involvement of CD9 and PDGFR in migration is evolutionarily conserved from *Drosophila* glia to human glioma. *Lab. Invest.* **124**, 373–383
25. Luo, B. H., Carman, C. V., and Springer, T. A. (2007) Structural basis of integrin regulation and signaling. *Annu. Rev. Immunol.* **25**, 619–647
26. Campbell, I. D., and Humphries, M. J. (2011) Integrin structure, activation, and interactions. *Cold Spring Harb. Perspect. Biol.* **3**, a004994
27. Seetharaman, S., and Etienne-Manneville, S. (2018) Integrin diversity brings specificity in mechanotransduction. *Biol. Cell* **110**, 49–64
28. Humphries, M. J. (2000) Integrin structure. *Biochem. Soc. Trans.* **28**, 311–339
29. Holmblad, T., Thörnqvist, P. O., Söderhäll, K., and Johansson, M. W. (1997) Identification and cloning of an integrin beta subunit from hemocytes of the freshwater crayfish *Pacifastacus leniusculus*. *J. Exp. Zool.* **277**, 255–261
30. Burke, R. D. (1999) Invertebrate integrins: Structure, function, and evolution. *Int. Rev. Cytol.* **191**, 257–284
31. Dinkins, M. B., Fratto, V. M., and Lemosy, E. K. (2008) Integrin alpha chains exhibit distinct temporal and spatial localization patterns in epithelial cells of the *Drosophila* ovary. *Dev. Dyn.* **237**, 3927–3939
32. O'Reilly, A. M., Lee, H. H., and Simon, M. A. (2008) Integrins control the positioning and proliferation of follicle stem cells in the *Drosophila* ovary. *J. Cell Biol.* **182**, 801–815
33. Yee, G. H., and Hynes, R. O. (1993) A novel, tissue-specific integrin subunit, beta nu, expressed in the midgut of *Drosophila melanogaster*. *Development* **118**, 845–858
34. Lavine, M. D., and Strand, M. R. (2003) Hemocytes from *Pseudoplusia includens* express multiple alpha and beta integrin subunits. *Insect Mol. Biol.* **12**, 441–452
35. Levin, D. M., Breuer, L. N., Zhuang, S., Anderson, S. A., Nardi, J. B., and Kanost, M. R. (2005) A hemocyte-specific integrin required for hemocytic encapsulation in the tobacco hornworm, *Manduca sexta*. *Insect Biochem. Mol. Biol.* **35**, 369–380
36. Lanot, R., Zachary, D., Holder, F., and Meister, M. (2001) Postembryonic hematopoiesis in *Drosophila*. *Dev. Biol.* **230**, 243–257
37. Lebestky, T., Chang, T., Hartenstein, V., and Banerjee, U. (2000) Specification of *Drosophila* hematopoietic lineage by conserved transcription factors. *Science* **288**, 146–149
38. Junkunlo, K., Söderhäll, K., and Söderhäll, I. (2019) Transglutaminase inhibition stimulates hematopoiesis and reduces aggressive behavior of crayfish, *Pacifastacus leniusculus*. *J. Biol. Chem.* **294**, 708–715
39. Junkunlo, K., Söderhäll, K., Söderhäll, I., and Noonin, C. (2016) Reactive oxygen species affect transglutaminase activity and regulate hematopoiesis in a crustacean. *J. Biol. Chem.* **291**, 17593–17601
40. Lin, X., and Söderhäll, I. (2011) Crustacean hematopoiesis and the astakine cytokines. *Blood* **117**, 6417–6424
41. Luo, H., Hanratty, W. P., and Dearolf, C. R. (1995) An amino acid substitution in the *Drosophila* hopTum-1 Jak kinase causes leukemia-like hematopoietic defects. *EMBO J.* **14**, 1412–1420
42. Munier, A. I., Doucet, D., Perrodou, E., Zachary, D., Meister, M., Hoffmann, J. A., Janeway, C. A., Jr., and Lagueux, M. (2002) PVF2, a PDGF/VEGF-like growth factor, induces hemocyte proliferation in *Drosophila* larvae. *EMBO Rep.* **3**, 1195–1200
43. Brown, S., Hu, N., and Hombria, J. C. (2001) Identification of the first invertebrate interleukin JAK/STAT receptor, the *Drosophila* gene domeless. *Curr. Biol.* **11**, 1700–1705
44. Li, D., Wan, Z., Li, X., Duan, M., Yang, L., Ruan, Z., Wang, Q., and Li, W. (2019) Alternatively spliced down syndrome cell adhesion molecule

Invertebrate IL-16 regulates hemocyte proliferation

- (Dscam) controls innate immunity in crab. *J. Biol. Chem.* **294**, 16440–16450
45. Santos, H. M., Tsai, C. Y., Maquiling, K. R. A., Tayo, L. L., Mariatulqabiah, A. R., Lee, C. W., and Chuang, K. P. (2020) Diagnosis and potential treatments for acute hepatopancreatic necrosis disease (AHPND): A review. *Aquac. Int.* **28**, 169–185
46. Yang, L., Li, X., Qin, X., Wang, Q., Zhou, K., Li, H., Zhang, X., Wang, Q., and Li, W. (2019) Deleted in azoospermia-associated protein 2 regulates innate immunity by stimulating Hippo signaling in crab. *J. Biol. Chem.* **294**, 14704–14716
47. Wang, X. W., Zhao, X. F., and Wang, J. X. (2014) C-type lectin binds to β -integrin to promote hemocytic phagocytosis in an invertebrate. *J. Biol. Chem.* **289**, 2405–2414